Adaptive Digital Press Optimization via Intelligent Calibration System

Chunghui Kuo; Eastman Kodak Company, 2600 Manitou Road, Rochester, NY 14653, USA

Abstract

Digital printing has begun to play an ever-increasing role in the commercial printing industry. The usual approach to tackle all imaging artifacts is to optimize each subsystem and hope the final assembled system will satisfy the product requirement. While the subsystem optimization is necessary, it might result in overstringent requirements for each subsystem, but still not address the problems from the interaction among subsystems. An efficient optimization process to compensating the residual image artifacts on an assembled printing press will address this deficiency to further reduce system manufacturing constraints and extend the life expectancy of imaging components. The Intelligent Calibration System is an adaptive digital press optimization process to address one-dimensional macro nonuniformity and color-to-color misregistration using its digital writing module and a fast image-capturing device.

Introduction

As digital printing technologies, such as electrophotography, drop-on-demand inkjet, and continuous inkjet, gradually broaden their service in the commercial printing industry, the demand for their capabilities to deliver high-quality prints with lower cost has persistently increased. A digital press is composed of many subsystems, and each subsystem can potentially contribute to imaging artifacts. The usual approach to tackle any artifact on a digital press is to optimize each subsystem and hope the final assembled system will satisfy the product requirement. While the subsystem optimization is necessary to improve the overall system performance in image quality, it might result in a very stringent requirement for each subsystem because of the effect of accumulating error in the final system. Furthermore, the subsystem optimization process does not address problems arising from interactions among subsystems. As a result, an efficient optimization process with the capability to compensate residual image artifacts on an assembled printing press will provide several advantages to assist the current digital press development process and benefit press customers, such as reduced system manufacturing constraints, extended life expectancy of imaging components, reduced running cost, and shorter artifact-recovery time [1, 2, 3].

The *Intelligent Calibration System* is an adaptive digital press optimization process that addresses the artifacts of one-dimensional macro nonuniformity and color-to-color misregistration using its digital writing module and a fast image-capturing device. One-dimensional macro nonuniformity, often denoted as streaking or banding depending on its periodicity characteristics, has long plagued digital printing systems, and can be caused by any subsystem, by the interaction among subsystems and printed substrates, and by image content. Because of its unpredictable nature, an active signal cancellation-like process, denoted as the calibration process, might be better equipped to handle this artifact [1, 3, 4]. In general, the calibration process can either adopt an actual signal-generation device, such as a Laser or LED writer, or perform pixel correction on the intended virtual document. These proposed technologies have one similarity in their iterative nature with a feedback loop control scheme. That is, the difference between the intended level and the actual measured level, denoted as δy_0 in a chosen color space, is estimated, and then used to drive the calibration process to reduce the difference. Gradually, $|\delta y_i|$, $i = 1 \cdots k$, should decrease with properly chosen feedback control parameters. These techniques, denoted as recursive compensation processes, assume little or no prior knowledge regarding the underlying printing process. While they can incrementally achieve the objective to reduce streaking and banding, it is more desirable and efficient to devise the deterministic compensation process that can precisely determine modification parameters based on a single acquired signal and knowledge of the adopted imaging process. The Intelligent Calibration System is a deterministic compensation process using the LED digital writing module as the compensating signal generator. While the electrophotographic printing process is assumed in this paper, it is possible to extend this deterministic compensation process to other printing processes.

The actual one dimensional nonuniformity signal $s_o(x,v)$ needs to be predicted at every spatial location x and pixel level v for the success of the signal cancellation algorithm. Hence, the capability to precisely locate any streak signal in the spatial domain can be readily extended to estimating and calibrating error in registration among different colors. The Intelligent Calibration System will first estimate the distance between two registration marks with different colors and their deviation from the theoretical positions. An over-determined linear system can be formulated by adopting different choices of color pairs and physical locations, and the corresponding least-square solution represents an estimation of the color registration error.

Intelligent Calibration System

The Intelligent Calibration System adopts the LED writer to generate the inverse signal

$$\kappa(x,v) = \psi^{-1}(\mu_o(x,v) - \bar{s}_o(x,v)), \tag{1}$$

where $\bar{s}_o(x,v)$ is the estimate of the unknown one-dimensional nonuniformity signal $s_o(x,v)$ based on a single scanned target and $\mu_o(x,v)$ is the aimed color at location x and pixel level v. $\psi(\kappa(x,v))$ represents the mapping function from the exposure level, $\kappa(x,v)$, of the LED writer to the perceived color on the printed substrate [5, 6, 7, 8]. In the scenario where $s_o(x,v) = 0$, $\kappa_o(x,v) = \psi^{-1}(\mu_o(x,v))$ is the a-priori LED uniformity correc-

tion. Denote the measured nonuniformity signal as $y(x,v)$, and assume that

$$y(x,v) = \phi(s_o(x,v)) + e(x,v), \tag{2}$$

where $\phi(\cdot)$ represents the mapping function from printing and image capturing processes and $e(x,v)$ is the associated random noise. $\phi(\cdot)$ can be affected by, printing halftone patterns, toner physical properties, the transfer function of the chosen image capturing device, etc. $\bar{s}_o(x,v)$ is the solution of the following minimization problem subject to certain smoothness and/or sparsity constraints, Γ:

$$\bar{s}_o(x,v) = \min_s \|\phi^{-1}(y(x,v)) - s(x,v)\|, \ \ \forall \ s(x,v) \in \Gamma. \tag{3}$$

For example, Γ could be the set of piecewise smooth functionals. Equation (2) becomes a traditional noise removal problem if $\phi(\cdot)$ becomes an identify function.

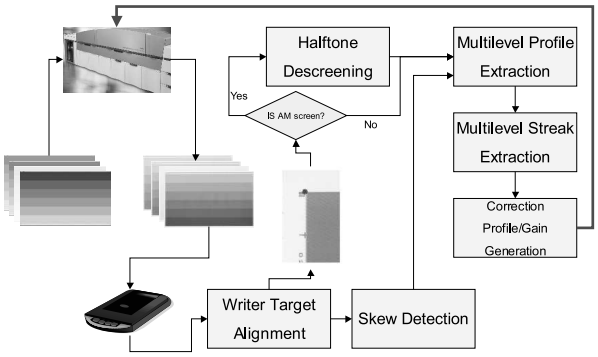

Figure 1. *The nonuniformity calibration in the Intelligent Calibration System.*

Uniformity Calibration

There exists two different ways to reproduce images on a substrate, i.e., halftone and continuous tone, and the color mixing theories to explain how light interacts with the substrate and colorant before reaching our eyes are slightly different [9]. The *Yule-Nielsen* model was proposed to explain the color mixing behavior in the halftone printing processing:

$$A_h^{(n)} = \frac{1 - 10^{-D/n}}{1 - 10^{-D_s/n}}, \tag{4}$$

where A_h is the halftone dot area, D_s is the reflection density of the solid patch of the selected color, D is the measured reflecting density of the halftone color patch, and n is determined by the actual printing process. In the extreme case of $n \to \infty$,

$$\tilde{A_h} = \frac{D}{D_s}. \tag{5}$$

Since the mapping from $A_h^{(n_1)}$ to $A_h^{(n_2)}$ is bijective, without loss of generality, we can focus the following analysis using $\tilde{A_h}$. As a result, we can deduce that the nonuniformity in reflection density on a halftone print sample, ΔD, is proportional to the variation in the dot area, $\Delta\tilde{A_h}$. Let r be the radius of a halftone dot, and $\tilde{A}_h = \pi r^2$. One unknown disturbance, ϑ_i, in the printing system drives the printing system away from its aimed reflection density at location x_i. We can deduce that ϑ_i results in small variation δr_i in the radius, r_i, of the halftone dot at x_i. That is:

$$r_i \to r_i + \delta r_i \tag{6}$$

where δr_i is a function of r_i. Based on the Taylor expansion, we can decompose δr_i as:

$$\delta r_i = \sum_{k=0}^{\infty} \alpha_{ik} r_i^k = \alpha_{i0} + \alpha_{i1} r_i + \rho(r_i) \approx \alpha_{i0} + \alpha_{i1} r_i, \tag{7}$$

where $\{\alpha_{ik}\}_{k=0}^{\infty}$ is determined by ϑ_i and $\rho(r_i)$ is assumed to be negligible since δr_i is usually very small. We can denote $\{\alpha_{i0}, \alpha_{i1}\}$ as streak coefficients at the location x_i. There exists three possible scenarios based on the sign of α_{i0}:

$\alpha_{i0} > 0$: This indicates detectable color tint at supposedly blank substrate location x_i, i.e., high background artifact.

$\alpha_{i0} < 0$: This nonuniformity will change its perceived polarity, for example, the streak might change from a light streak to a dark streak at location x_i.

$\alpha_{i0} = 0$: This nonuniformity is consistent in its perceived polarity.

In this paper, we will focus on the last case, and we can derive

$$\Delta D_i = D_s \Delta\tilde{A}_h = D_s 2\pi r_i \delta r_i = 2D_s \alpha_{i1} \pi r_i^2 = 2D_s \alpha_{i1} \tilde{A}_{hi}. \tag{8}$$

Equation (8) suggests that the magnitude of the streak signal ΔD_i at location x_i is linearly proportional to $\tilde{A}_{hi}$. Let $\vec{s}_j$ and $\vec{\alpha}$ be the estimated reflection density variation and the corresponding streak coefficients, $[\alpha_{11}, \alpha_{21}, \cdots, \alpha_{k1}]^T$ where k is the number of LEDs, across the full range at averaged colorant coverage $\tilde{A}_h^j$, where $j = 1 \cdots J$. Estimating $\vec{\alpha}$ from single realization of $\vec{s}_j$ and $\tilde{A}_h^j$ is noisy and unreliable. This problem can be greatly alleviated by correlating estimated reflection variation at multiple density levels as follows:

$$S = [\vec{s}_1 \ \vec{s}_2 \ \cdots \ \vec{s}_J] = 2D_s[\tilde{A}_h^1 \ \tilde{A}_h^2 \ \cdots \ \tilde{A}_h^J]\vec{\alpha}. \tag{9}$$

The above equation indicates that the rank of S is 1, and the remaining $J-1$ subspace is the null space spanned by printing and/or scanning noise. As a result, $\vec{\alpha} = |v|\vec{\eta}$, where $\vec{\eta}$ is the first singular vector of S. Each component $\vec{s}_j$ in S is obtained by solving Equation (3). We can further simplify the problem by assuming $\phi(\cdot)$ is an identity function if the selected halftone screen is capable of reproducing fine details and the Modulation Transfer Function of the chosen image capturing device is close to an all-pass filter. A stationary wavelet transform with soft thresholding is adopted to derive the optimal estimation of $\vec{s}_j$ at each coverage $\tilde{A}_h^j$. Hence, the one-dimensional nonuniformity is governed by:

$$S = 2D_s[\tilde{A}_h^1 \ \tilde{A}_h^2 \ \cdots \ \tilde{A}_h^J]|v|\vec{\eta}. \tag{10}$$

It is necessary to establish the relationship between $\vec{\alpha}$ and $\vec{\kappa}$, $\psi^{-1}(\cdot)$, as described in Equation (1), which depends on the chosen printing process. We will focus on the *electrophotographic* process in this paper. Assuming the thickness of the colorant layer

is fixed before multiple layers of colorant being formed on the substrate, we can deduce that $\tilde{A}_{hi}$ is proportional to M/A, which represents the colorant mass per unit area. M/A can subsequently be controlled by the LED writer. The theoretical analysis on the electrophotographic process using conductive magnetic brush development can be approximated in first order by the following equation [10]:

$$\tilde{A}_h \propto \frac{M}{A} = \frac{C_t \nu V p}{Q/M} \frac{\rho_c}{\rho_t} \frac{8\varepsilon_0}{r_t} = \beta_D V \tag{11}$$

where C_t is the toner concentration, ν is the speed ratio factor between roller and photoreceptor, V is the applied voltage, p represents carrier surface packing, Q/M is the charge-to-mass ratio, ρ_c and ρ_t are the densities of carrier and toner respectively, ε_0 is the permittivity of free space, and r_t stands for the toner radius. $\varphi(\kappa)$ represents the known mapping function from the exposure of the LED writer, κ, to the applied voltage, V, on the photoreceptor. As a result, we can derive the following relationship:

$$\begin{aligned} \frac{\Delta\tilde{A}_h}{\tilde{A}_h} &= \frac{2\delta r}{r} = 2\vec{\alpha} \propto \frac{\delta V}{V} = \frac{\delta\varphi(\kappa)}{\varphi(\kappa_o)} \\ &\Rightarrow \quad \delta\varphi(\kappa) \propto \vec{\alpha}\varphi(\kappa_o) \end{aligned} \tag{12}$$

Equation (12) summarizes the theoretical basis to deterministically correct one-dimensional nonuniformity by modifying the digital writing module, and the calibration algorithm is illustrated in Figure 1.

Color Registration Calibration

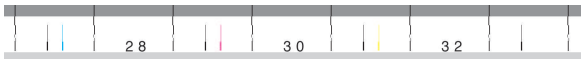

Figure 2. *The pairwise color fiducial marks.*

The most basic approach to precise measure registration error among different colors is to measure the position of each fiducial mark under high magnification and free of substrate deformation, and the distance between two fiducial marks, d_{c12}, satisfies

$$d_{c12} = p_{c2} - p_{c1}, \;\; p_{c2} > p_{c1}, \tag{13}$$

where p_{c1} and p_{c2} are the fiducial positions of $color1$ and $color2$. The difficulty arises when there is constraint on the magnification level and unpredictable substrate deformation. Both problems need to be addressed in the *Intelligent Calibration System*. The designed target to measure registration is shown in Figure 2. The periodic positional marks are used to calibrate deformation of the digitally captured target, where the distance between two neighboring positional marks is known. The relative positions of two color fiducial marks are measured relative to the two closest positional marks. This is the first step to reduce measurement error. Second, the same pair of color fiducial marks, for example cyan and magenta, will occur multiple times on the same captured target, and the average distance between them is adopted to further reduce the measurement error. In the case of N-color printing, there are $N(N-1)$ two-color combinations. Hence, we can form the same number of linear equations according Equation (13) with the unknown being the location of each color channel. This is an over-determined linear system, $H\vec{p} = \vec{d}$, where $H \in \mathbf{Z}^{N(N-1)\times N}$, $\vec{p} \in \mathbf{R}^{N\times 1}$, and $\vec{d} \in \mathbf{R}^{N(N-1)\times 1}$. Hence,

$$\vec{p} = (H^T H)^{-1} H^T \vec{d}. \tag{14}$$

Experimental Result

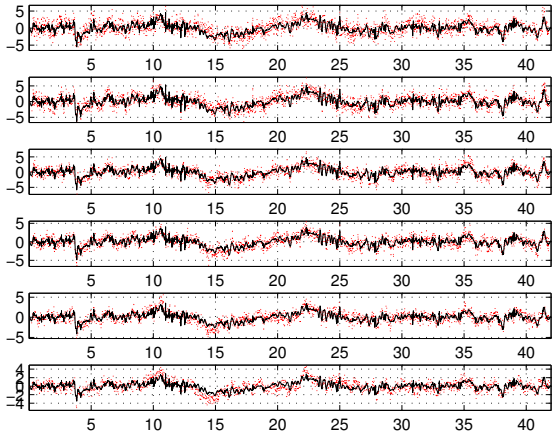

Figure 3. *The measured nonuniformity signals (dashed line) and their corresponding model fit (solid line).*

Figure 1 summarizes the nonuniformity calibration algorithm in the Intelligent Calibration System. After the printed target is captured by a document scanner, the positional marks along the top and bottom of the target are identified to serve as the spatial references. The profile extraction algorithm uses these spatial references to estimate the signal strength of nonuniformity across the LED pixel locations at each $\tilde{A}_h$ level. The resulting nonuniformity signals after the multilevel streak extraction module, which adopts the stationary wavelet transform with soft-thresholding technique to remove measurement noise, are shown in Figure 3. Six levels of $\tilde{A}_h$ are included in the designed target, and the relative strength of the singular values of the nonuniformity signal matrix, $S \in \mathbf{R}^{8064\times 6}$, shown in Figure 4, indicates that the rank of S can be treated being one as suggested in Equation (10). ν can be estimated from the slope of the linear fit as shown in Figure 4, and the corresponding LED power modification percentage based on this scanned target is shown in Figure 5.

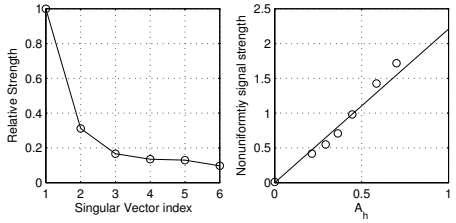

Figure 4. *Rank estimation of S and the proposed linear model fit for nonuniformity signals at different $\tilde{A}_h$.*

The Intelligent Calibration System uses a document scanner as the image capturing device to scan images while transporting

substrate using rollers. Therefore, the spatial scanning accuracy can be insufficient to satisfy the high-precision requirement of the color registration calibration. Figure 6 shows the measured signal of the positional marks and color fiducial marks. The actual distance between two positional marks should be 192 pixels, but the measured distance between them ranges from 188 to 194 pixels with overall average distance being less than 192. Hence, the procedure suggested in previous sections is necessary to achieve needed accuracy for precise color registration control. Figure 7 demonstrates the results of before and after color registration calibration.

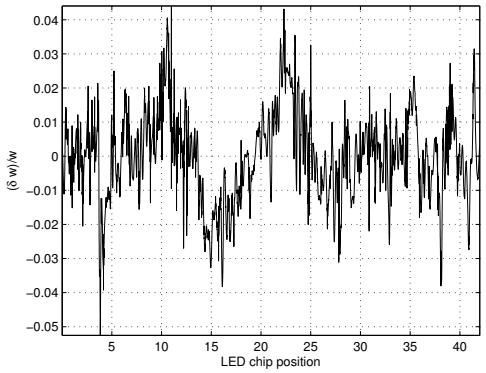

Figure 5. *LED exposure modification.*

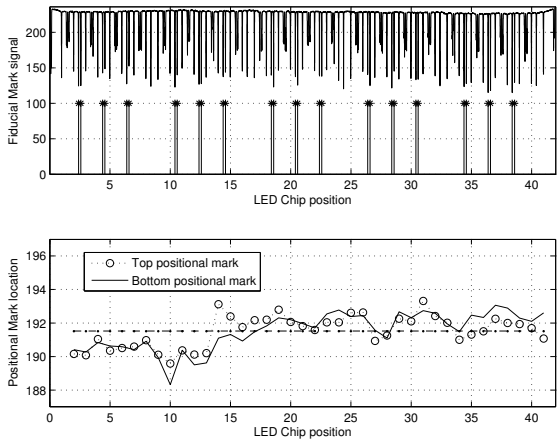

Figure 6. *The estimated positional mark and color fiducial mark positions.*

Conclusion

A deterministic compensation process, the Intelligent Calibration System, calibratew color nonuniformity and registration artifacts. This system has been deployed in the field and shown its effectiveness to address the targeted artifacts. Furthermore, since this system actively compensates for color nonuniformity, it reduces the frequency of unnecessary or immature imaging component replacement, which, in turn, results in higher uptime for the printing press and cost savings for the customers.

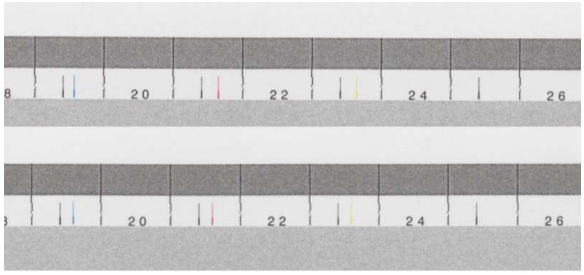

Figure 7. *Color fiducial marks before and after registration calibration.*

References

[1] A. Rushing and Y. Ng, *Scanner as test print densitometer for compensating overall process drift and nonuniformity*, US Patent 5,546,165, August 1996.

[2] E. C. Stelter, K. P. Friedrich, and J. Guth, *Reduction of Banding and Mottle in Electrophotographic Systems*, US Patent 6,885,833, April 2005

[3] M. Sampath, H. Mizes, and S. Zoltner, *Methods and system for automatically compensating for diagnosed banding defects prior to the performance of remedial service*, US Patent 7,400,339, July 2008.

[4] H. Mizes, et. al., *Automatic Density Control for Increased Print Uniformity and Printer Reliablity with Inline Linear Array Sensing*, pp. 206 - 210, IS&T NIP24, September 2008.

[5] H. Tai, *Apparatus and Methods for Calibrating a Gray Level Printhead*, US Patent 5,200,765, April 1993.

[6] H. Hamano et. al., *1200 DPI LED Printhead for Very High Speed Printing*, pp. 405 - 408, IS&T NIP14, September 1998.

[7] I. Ajewole and Y. Ng, *Quasi-Center-Weighted PWM Multi-Level LED Printhead with Non-Linear Exposure Uniformity Correction*, pp. 287 - 292, IS&T NIP16, September 2000.

[8] M. Ogihara et. al., *New Printhead Using LED Arrays Integrated with IC Drivers*, pp. 402 - 405, IS&T NIP22, September 2006.

[9] H. R. Kang, *Digital Color Halftoning*, The Society of Photo-Optical Instrumentation Engineers, 1999.

[10] L. B. Schein, *ElectroPhotography and Development Physics*, Revised 2nd ed., Laplacian Press, 1999

Author Biography

Chunghui Kuo is a Scientist at Eastman Kodak Company. He received his Ph.D. in Electrical and Computer Engineering from the University of Minnesota and joined Kodak in 2001. His research interest is in image processing, image quality, blind signal separation and classification, and neural network applied in signal processing. He is a senior member of the IEEE Signal Processing Society and a member of IS&T.